protein structure communications

Acta Crystallographica Section F
Structural Biology and Crystallization Communications

ISSN 1744-3091

Crystallization and X-ray diffraction analysis of N-terminally truncated human ALG-2

Hironori Suzuki,[a] Masato Kawasaki,[b] Takeshi Kakiuchi,[a] Hideki Shibata,[a] Soichi Wakatsuki[b] and Masatoshi Maki[a]*

[a]Department of Applied Molecular Biosciences, Graduate School of Bioagricultural Sciences, Nagoya University, Nagoya 464-8601, Japan, and [b]Structural Biology Research Center, Photon Factory, Institute of Materials Structure Science, High Energy Accelerator Research Organization (KEK), Tsukuba, Ibaraki 305-0801, Japan

Correspondence e-mail: mmaki@agr.nagoya-u.ac.jp

Received 5 August 2008
Accepted 20 September 2008

PDB References: ALG-2, Ca^{2+}-bound form, 2zrs, r2zrssf; Zn^{2+}-bound form, 2zrt, r2zrtsf.

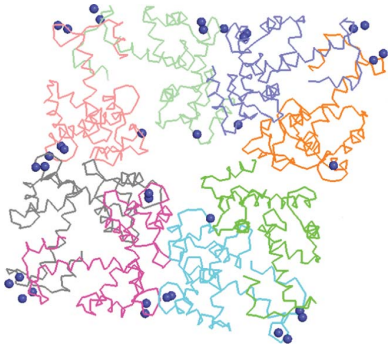

ALG-2 (apoptosis-linked gene 2) is an apoptosis-linked calcium-binding protein with five EF-hand motifs in the C-terminal region. N-terminally truncated ALG-2 (des3-23ALG-2) was crystallized by the vapour-diffusion method in buffer consisting of either 50 m*M* MES pH 6.5, 12.5%(*v*/*v*) 2-propanol and 150 m*M* calcium acetate or 100 m*M* MES pH 6.0, 15%(*v*/*v*) ethanol and 200 m*M* zinc acetate. Crystals of the Ca^{2+}-bound form belonged to space group $P2_12_12_1$, with unit-cell parameters a = 54.8, b = 154.4, c = 237.7 Å, $\alpha = \beta = \gamma = 90^\circ$, and diffracted to 3.1 Å resolution. Crystals of the Zn^{2+}-bound form belonged to space group $P2_12_12_1$, with unit-cell parameters a = 52.8, b = 147.5, c = 230.7 Å, $\alpha = \beta = \gamma = 90^\circ$, and diffracted to 3.3 Å resolution. The structures of the Ca^{2+}-bound form and the Zn^{2+}-bound form were solved by the molecular-replacement method. Although both crystals contained eight ALG-2 molecules per asymmetric unit, the metal-ion locations and octameric arrangements were found to be significantly different.

1. Introduction

ALG-2 (apoptosis-linked gene 2) is a 22 kDa calcium-binding protein that contains five EF-hand motifs (EF1–EF5) in its C-terminal region and belongs to the penta-EF-hand (PEF) family, which includes conventional calpains, sorcin, grancalcin and peflin in mammals (for reviews, see Maki *et al.*, 1997, 2002). With the exception of the calpain large subunit, PEF family proteins have various lengths of Gly/Pro-rich hydrophobic regions in their N-terminal regions (human ALG-2: 1-MAAYSYRPGPGAGPGPAAGAALP-23). ALG-2 and its interacting protein Alix/AIP1 have been suggested to function in apoptosis, development and cancer (Vito *et al.*, 1996; Sadoul, 2006; Maki & Shibata, 2007). ALG-2 exists as a weak dimer in solution in the absence of Ca^{2+} (Lo *et al.*, 1999) and forms a homodimer or a heterodimer with another PEF protein, peflin, through their EF5 regions (Kitaura *et al.*, 2001, 2002). However, in the presence of Ca^{2+} ALG-2 undergoes a conformational change that exposes its hydrophobic surfaces and precipitates at high protein concentrations (Maki *et al.*, 1998). The Ca^{2+}-bound form of elastase-treated mouse ALG-2 (des1-20ALG-2) has been solved (PDB code 1hqv; Jia *et al.*, 2001) and we have recently reported the structures of the Ca^{2+}-bound form of N-terminally truncated human ALG-2 (des3-20ALG-2) and the

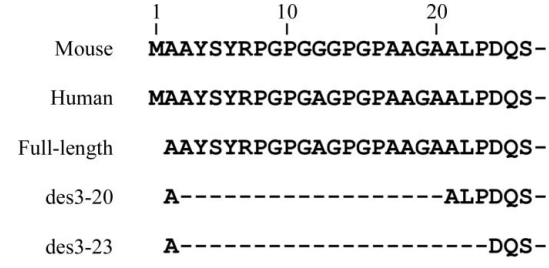

Figure 1
N-terminal sequences of mouse and human ALG-2. There are two amino-acid substitutions between mouse and human ALG-2 in the full-length sequence of 191 residues (Gly12 and Gln46 in mouse *versus* Ala12 and Thr46 in human). We have previously crystallized the full-length ALG-2 protein and the N-terminal deletion mutant des3-20ALG-2. In this study, we crystallized des3-23ALG-2.

Zn^{2+}-bound form of full-length ALG-2 (Suzuki *et al.*, 2008). Here, we report the crystallization and X-ray diffraction analysis of Ca^{2+}-bound and Zn^{2+}-bound forms of human ALG-2 with a deletion of amino-acid residues 3–23 (des3-23ALG-2; Fig. 1). Both crystals contain eight ALG-2 molecules in the asymmetric unit, but the metal-ion locations and octameric arrangements were found to differ significantly between crystals grown in the presence of Ca^{2+} or Zn^{2+}.

2. Materials and methods

2.1. Expression and purification

Construction of an expression plasmid for untagged but N-terminally truncated human ALG-2 that lacks the Gly/Pro-rich hydrophobic region, designated ALG-2ΔN23, has been described previously (Satoh *et al.*, 2002) and is renamed des3-23ALG-2 here (Fig. 1). The des3-23ALG-2 protein was expressed and purified using an affinity column in which a phospholipid scramblase 3 (PLSCR3) oligopeptide, a Ca^{2+}-dependent ALG-2-interacting peptide, was immobilized and the bound protein in the presence of Ca^{2+} was eluted with a solution of the calcium chelator EGTA essentially as described previously (Shibata *et al.*, 2008). After affinity purification, 2 ml of the ALG-2 protein solution was dialyzed first against 2 l of 2 m*M* Tris–HCl pH 7.5 containing 1 m*M* each of EDTA and EGTA and then twice against 2 l of 2 m*M* Tris–HCl pH 7.5 containing 2 µ*M* each of EDTA and EGTA. Proteins were then concentrated to about 10 mg ml^{-1} using a vacuum centrifuge evaporator (Sakuma, Japan). Finally, the concentrated proteins were dialyzed against 10 m*M* Tris–HCl pH 7.5 containing 10 µ*M* each of EDTA and EGTA.

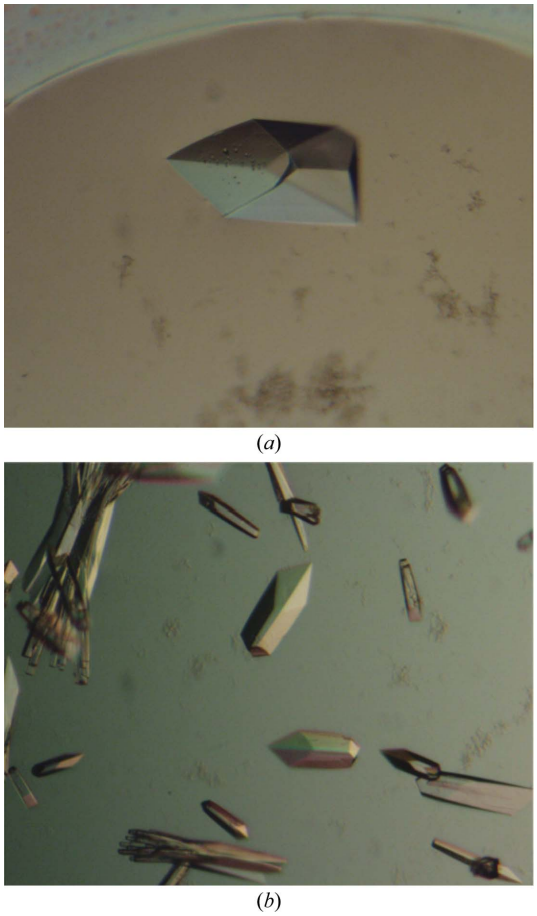

(*a*)

(*b*)

Figure 2
Photomicrographs of des3-23ALG-2 crystals. (*a*) Ca^{2+}-bound form, (*b*) Zn^{2+}-bound form.

Table 1
Data-collection, processing and refinement statistics.

Values in parentheses are for the highest resolution shell.

	Ca^{2+}-bound	Zn^{2+}-bound
PDB code	2zrs	2zrt
Data collection		
Space group	$P2_12_12_1$	$P2_12_12_1$
Unit-cell parameters		
a (Å)	54.8	52.8
b (Å)	154.4	147.5
c (Å)	237.7	230.7
$\alpha = \beta = \gamma$ (°)	90	90
X-ray source	PF BL-5A	Spring-8 BL41XU
Wavelength (Å)	1.0000	1.2819
Temperature (K)	100	100
Resolution (Å)	50–3.1 (3.2–3.1)	50–3.3 (3.4–3.3)
Observed reflections	263300	243748
Unique reflections	37803	27970
Completeness (%)	100.0 (98.4)	99.5 (96.6)
R_{merge}† (%)	9.4 (30.9)	10.2 (34.3)
$\langle I/\sigma(I)\rangle$	6.7 (4.6)	8.0 (2.9)
Refinement		
R_{work}/R_{free}‡(%)	22.8/28.0	16.9/22.1
Average B factor (Å^2)	42.06	99.31
R.m.s.d. bond lengths (Å)	0.008	0.006
R.m.s.d. bond angles (°)	1.138	0.890
No. of atoms	10956	11010

† $R_{merge} = \sum_{hkl}\sum_i |I_i(hkl) - \langle I(hkl)\rangle| / \sum_{hkl}\sum_i I_i(hkl)$, where $I_i(hkl)$ is the ith measurement of reflection indices hkl and $\langle I(hkl)\rangle$ is the mean intensity. ‡ $R_{work} = \sum_h ||F_o(h)| - |F_c(h)|| / \sum_h |F_o(h)|$; R_{free} was calculated using 10% of data excluded from refinement.

2.2. Crystallization

Initial crystallization trials were performed with crystallization reagent kits from Hampton Research (Crystal Screens 1 and 2, PEG/Ion Screen, Natrix and MembFac), from Emerald BioStructures (Wizard I and II, Cryo I and II) and from Molecular Dimensions (Stura Footprint Screens) by the sitting-drop vapour-diffusion method at 293 K using an automatic crystallization robot system (Hiraki *et al.*, 2006). Drops containing 0.5 µl protein sample (10 mg ml^{-1}) and 0.5 µl reservoir solution were equilibrated against 180 µl reservoir solution. Crystals of des3-23ALG-2 were obtained using Wizard I condition No. 40 [100 m*M* MES pH 6.0, 10%(*v*/*v*) 2-propanol, 200 m*M* calcium acetate] and Wizard II condition No. 20 [100 m*M* MES pH 6.0, 15%(*v*/*v*) ethanol, 200 m*M* zinc acetate] and crystallization conditions were optimized manually by the hanging-drop vapour-diffusion method. In the final crystallization conditions, the Ca^{2+}-bound form of des3-23ALG-2 was crystallized using 50 m*M* MES pH 6.5 containing 12.5%(*v*/*v*) 2-propanol and 150 m*M* calcium acetate (Fig. 2*a*). The Zn^{2+}-bound form of des3-23ALG-2 was crystallized under the same conditions using Wizard II condition No. 20 [100 m*M* MES pH 6.0, 15%(*v*/*v*) ethanol, 200 m*M* zinc acetate] (Fig. 2*b*).

2.3. Data collection and refinement

Data collection was performed on BL-5A at The Photon Factory (Tsukuba, Japan) and on BL41XU at SPring-8 (Harima, Japan). The crystals were soaked for a few seconds in reservoir solution containing 20% glycerol. Crystals were then picked up with nylon-fibre loops and flash-cooled in a nitrogen-gas stream. The diffraction data were indexed, integrated and scaled with the *HKL*-2000 program package (Otwinowski & Minor, 1997). The phase problem

was solved by the molecular-replacement method with the program *MOLREP* (Vagin & Teplyakov, 1997) using the structure of elastase-treated N-terminally truncated mouse ALG-2 (PDB code 1hqv; Jia *et al.*, 2001) as a search model. The X-ray data statistics are shown in Table 1. Both models were refined using the programs *CNS* (Brünger *et al.*, 1998) and *REFMAC*5 (Murshudov *et al.*, 1997). The models were manually adjusted using *Coot* (Emsley & Cowtan, 2004).

3. Results and discussion

The crystals of des3-23ALG-2 grown in the buffer containing calcium acetate belonged to space group $P2_12_12_1$, with unit-cell parameters $a = 54.8$, $b = 154.4$, $c = 237.7$ Å, $\alpha = \beta = \gamma = 90^\circ$, and diffracted to 3.1 Å resolution. Specific volume calculations based on the unit-cell parameters and the molecular weight (the Matthews coefficient; Matthews, 1968) suggested that there could be eight ALG-2 molecules per asymmetric unit, with a V_M value of 2.8 Å^3 Da^{-1} and a solvent content of 61.1%. The crystals grown in the buffer containing zinc acetate also belonged to space group $P2_12_12_1$, with unit-cell parameters $a = 52.8$, $b = 147.5$, $c = 230.7$ Å, $\alpha = \beta = \gamma = 90^\circ$, and diffracted to 3.3 Å resolution. The Matthews coefficient suggests the presence of eight ALG-2 molecules in the asymmetric unit (V_M = 2.8 Å^3 Da^{-1}; 56.5% solvent content). Although only seven ALG-2 molecules were obtained by molecular replacement with the Ca^{2+}-bound structure of elastase-treated mouse ALG-2 (PDB code 1hqv; Jia *et al.*, 2001) as a search model, the eighth ALG-2 molecule was assigned during the course of refinement. ALG-2 formed a homodimer and four homodimers (molecules *AB*, *CD*, *EF* and *GH*) are arranged in a pseudo-screw along the *a* axis (Fig. 3). A comparison of the resolved structures (PDB codes: Ca^{2+}-bound form, 2zrs; Zn^{2+}-bound form, 2zrt) revealed differences in the octameric arrangements (Fig. 3) and metal-ion locations (Table 2). According to the crystal packing (Fig. 3) and the solvent contents from V_M calculations, the Zn^{2+}-bound form seems to be better packed than the Ca^{2+}-bound form. However, the overall *B* factor of the Ca^{2+}-bound form (42.1 Å^2) was lower than that of the Zn^{2+}-bound form (99.3 Å^2). This may explain why the crystals of the Ca^{2+}-bound form diffracted to higher resolution than those of the Zn^{2+}-bound form.

Using different recombinant proteins, we were able to solve the structures of the Ca^{2+}-bound form of des3-20ALG-2 and the Zn^{2+}-bound form of full-length ALG-2 at better resolutions (PDB codes: Ca^{2+}-bound form, 2zn9; Zn^{2+}-bound form, 2zn8; Suzuki *et al.*, 2008). These crystals were obtained in buffer consisting of either 100 m*M*

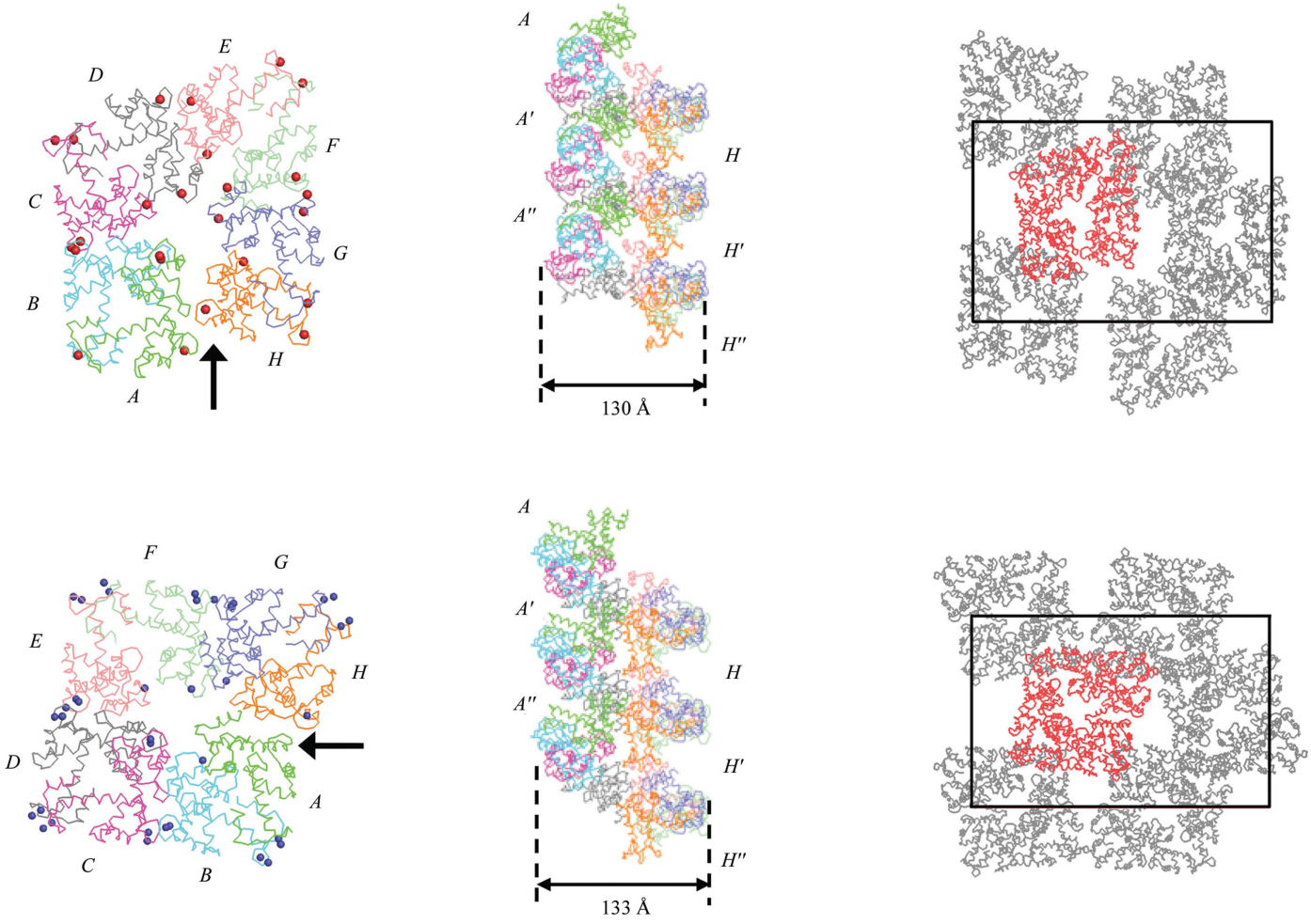

Figure 3
Overall structure in the asymmetric unit (left) and crystal packing (right) of the Ca^{2+}-bound form (top) and Zn^{2+}-bound form (bottom) of des3-23ALG-2 viewed from the *a* axis. Three stacked octamers (middle) are viewed along the *a* axis from the direction of the arrows indicated in the left panels. In the left and middle panels, the des3-23ALG-2 molecules are coloured as follows: molecule *A*, green; molecule *B*, cyan; molecule *C*, magenta; molecule *D*, grey; molecule *E*, pink; molecule *F*, lime; molecule *G*, blue; molecule *H*, orange. Calcium and zinc ions are shown as red and blue spheres, respectively, in the left panels. In the right panels the des3-23ALG-2 molecules are displayed in grey, except for the molecules in asymmetric unit, which are coloured red. Unit cells are depicted by black boxes. Diameters of psuedo-screws are indicated by arrow-headed bars.

Table 2
Numbers of calcium ions and zinc ions at EF1, EF3 and EF5.

Calcium ions and zinc ions are found intermolecularly coordinated to the Asn106 residues of two adjacent ALG-2 molecules (between molecules *B* and *C* and between molecules *F* and *G* in the Ca^{2+}-bound form and between molecules *B* and *C* and between molecules *D* and *E* in the Zn^{2+}-bound form).

	Calcium ions			Zinc ions		
	EF1	EF3	EF5	EF1	EF3	EF5
A	1	1	0	0	0	2
B	1	1	1	1	2	2
C	1	1	1	1	2	2
D	1	1	1	1	2	2
E	1	1	1	1	2	2
F	1	1	1	1	2	2
G	1	1	1	1	2	2
H	1	1	1	0	1	2

sodium cacodylate pH 6.5, 18%(*w*/*v*) PEG 8000 and 200 m*M* calcium acetate (Ca^{2+}-bound form) or 100 m*M* sodium cacodylate pH 6.5, 25%(*w*/*v*) MPD (2-methyl-2,4-pentanediol) and 75 m*M* zinc acetate (Zn^{2+}-bound form). They belonged to space groups $P4_1$ and $C222_1$ and diffracted to 2.4 and 2.7 Å resolution, respectively. Jia *et al.* (2001) previously crystallized mouse ALG-2 (des1-20ALG-2) using 100 m*M* sodium cacodylate pH 6.5, 12–15% PEG 8000 and 100 m*M* calcium acetate (space group $P4_122$) and determined the structure to 2.3 Å resolution. The organic precipitant may be involved in determining the Bravais lattice (ethanol and 2-propanol, primitive orthorhombic; PEG, primitive tetragonal; MPD, *C*-centred orthorhombic), as all the ALG-2 crystals described above were grown under similar conditions except for differences in the organic precipitant. Further truncation of the N-terminal sequence by three residues (21-AAP-23), which are located near the loop between EF3 and EF4 in the structures of the Ca^{2+}-bound forms of both human des3-20ALG-2 (PDB code 2zn9) and mouse des1-20ALG-2 (PDB code 1hqv), may have decreased the diffraction quality of the crystals obtained. We investigated the locations of the calcium and zinc ions (Table 2). These metal ions were found at EF1, EF3 and EF5 in most ALG-2 molecules, but molecule *A* lacks zinc ions at EF1 and EF3, whereas molecule *H* lacks a zinc ion at EF1. Surprisingly, both ions were also found intermolecularly in locations near the Asn106 residues of two adjacent ALG-2 molecules (between molecules *B* and *C* and between molecules *F* and *G* in the Ca^{2+}-bound form and between molecules *B* and *C* and between molecules *D* and *E* in the Zn^{2+}-bound form). Furthermore, we observed anomalous signals from Zn atoms and one extra zinc ion was found in the vicinity of the coordinated zinc ions at EF3 and EF5, with the exception of EF3 in molecule *H*. The smaller ionic radius of zinc (0.74 Å) compared with calcium (0.99 Å) may explain the binding of two zinc ions to EF5. The previously solved structure of the Zn^{2+}-bound form of full-length ALG-2 is very similar to that of the Ca^{2+}-bound form of des3-20ALG-2, with the exception of EF5 in which the relative position of α8 (exiting the EF5 helix) of the Zn^{2+}-bound form resembles that of the Ca^{2+}-free form (Suzuki *et al.*, 2008). Unfortunately, the resolutions of the structures of des3-23ALG-2 were not high enough to determine the metal-coordinating residues and quantitative comparisons with the previous structures could not be performed. Calcium ions bind to EF1 and EF3 of ALG-2 with a dissociation constant of 1.2 μ*M* (Tarabykina *et al.*, 2000). The binding ability of zinc ions to ALG-2 seems to be much weaker than that of calcium ions (Shibata *et al.*, 2008), suggesting that zinc ions do not bind to ALG-2 under physiological conditions. In conclusion, the crystal packing of ALG-2 is influenced by both the organic precipitants used in crystallization and the degree of truncation of the N-terminal sequence of ALG-2, resulting in differences in the metal-ion-binding pattern in the octameric structures and the quality of X-ray diffraction.

We thank Dr Hitomi (Nagoya University) and Dr Kato (KEK) for valuable suggestions. This work was partly supported by a Grant-in-Aid for Scientific Research (B) (to MM) and a Grant-in-Aid for JSPS Fellows (to HS) from JSPS.

References

Brünger, A. T., Adams, P. D., Clore, G. M., DeLano, W. L., Gros, P., Grosse-Kunstleve, R. W., Jiang, J.-S., Kuszewski, J., Nilges, M., Pannu, N. S., Read, R. J., Rice, L. M., Simonson, T. & Warren, G. L. (1998). *Acta Cryst.* D**54**, 905–921.
Emsley, P. & Cowtan, K. (2004). *Acta Cryst.* D**60**, 2126–2132.
Hiraki, M. *et al.* (2006). *Acta Cryst.* D**62**, 1058–1065.
Jia, J., Tarabykina, S., Hansen, C., Berchtold, M. & Cygler, M. (2001). *Structure*, **9**, 267–275.
Kitaura, Y., Matsumoto, S., Satoh, H., Hitomi, K. & Maki, M. (2001). *J. Biol. Chem.* **276**, 14053–14058.
Kitaura, Y., Satoh, H., Takahashi, H., Shibata, H. & Maki, M. (2002). *Arch. Biochem. Biophys.* **399**, 12–18.
Lo, K. W., Zhang, Q., Li, M. & Zhang, M. (1999). *Biochemistry*, **38**, 7498–7508.
Maki, M., Kitaura, Y., Satoh, H., Ohkouchi, S. & Shibata, H. (2002). *Biochim. Biophys. Acta*, **1600**, 51–60.
Maki, M., Narayana, S. V. & Hitomi, K. (1997). *Biochem. J.* **328**, 718–720.
Maki, M. & Shibata, H. (2007). *Calcium Binding Proteins*, **2**, 4–10.
Maki, M., Yamaguchi, K., Kitaura, Y., Satoh, H. & Hitomi, K. (1998). *J. Biochem.* **124**, 1170–1177.
Matthews, B. W. (1968). *J. Mol. Biol.* **33**, 491–497.
Murshudov, G. N., Vagin, A. A. & Dodson, E. J. (1997). *Acta Cryst.* D**53**, 240–255.
Otwinowski, Z. & Minor, W. (1997). *Methods Enzymol.* **276**, 307–326.
Sadoul, R. (2006). *Biol. Cell*, **98**, 69–77.
Satoh, H., Nakano, Y., Shibata, H. & Maki, M. (2002). *Biochim. Biophys. Acta*, **1600**, 61–67.
Shibata, H., Suzuki, H., Kakiuchi, T., Inuzuka, T., Yoshida, H., Mizuno, T. & Maki, M. (2008). *J. Biol. Chem.* **283**, 9623–9632.
Suzuki, H., Kawasaki, M., Inuzuka, T., Okumura, M., Kakiuchi, T., Shibata, H., Wakatsuki, S. & Maki, M. (2008). *Structure*. doi:10.1016/j.str.2008.07.012.
Tarabykina, S., Moller, A. L., Durussel, I., Cox, J. & Berchtold, M. W. (2000). *J. Biol. Chem.* **275**, 10514–10518.
Vagin, A. & Teplyakov, A. (1997). *J. Appl. Cryst.* **30**, 1022–1025.
Vito, P., Lacanà, E. & D'Adamio, L. (1996). *Science*, **271**, 521–525.